Kinetic Characterization and Identification of the Acylation and Glycosylation Sites of Recombinant Human γ-Glutamyltranspeptidase†

Roselyne Castonguay, Dany Halim, Mylène Morin, Alexandra Furtos, Christian Lherbet, Eric Bonneil, Pierre Thibault, and Jeffrey W. Keillor*

Département de chimie, Université de Montréal, Montréal, Québec, Canada H3C 3J7

Received May 18, 2007; Revised Manuscript Received August 24, 2007

ABSTRACT: γ-Glutamyltranspeptidase (GGT) is a heterodimeric enzyme important for glutathione homeostasis control. It has also been implicated in many physiological disorders, including Parkinson's disease, apoptosis inhibition, and diabetes. In the first step of its ping-pong mechanism it binds glutathione, its *in vivo* substrate, and releases cysteinylglycine upon formation of an acyl-enzyme intermediate. This intermediate can then react with water to release glutamate as a hydrolysis product or with an amino acid or dipeptide to form a transpeptidation product. Further detailed study of the mechanism underlying these reactions is hindered at least for some GGTs by the low quantities of protein available after a multistep purification from tissue. In the present work the gene for human GGT was cloned into the pPICZαA vector and transformed into *Pichia pastoris* to express as a 68 kDa His-tagged protein. The optimized expression and secretion of this enzyme in 1 L of culture and subsequent purification by immobilized metal affinity chromatography yielded 1.6 mg of purified enzyme having a specific activity of 237 U/mg. Kinetic parameters for the transpeptidation reaction between glutathione and glycylglycine were determined by mass spectrometry, giving a k_{cat} of 13.4×10^3 min^{-1} and apparent K_M values of 1.11 mM for glutathione and 8.1 mM for glycylglycine. The GGT-mediated hydrolysis of glutathione was also studied, providing a k_{cat} of 53 min^{-1} and a K_M value of 7.3 μM for glutathione. Incubation of the enzyme with a mechanism-based inhibitor, enzymatic digest, and mass spectrometric analysis provided the first unambiguous identification of Thr381 as the active site nucleophile of human γ-glutamyltranspeptidase, and confirmed four of the seven N-linked glycosylation sites. These structural and kinetic data are discussed with respect to a homology model generated to facilitate visualization.

γ-Glutamyltranspeptidase (GGT;[1] EC 2.3.2.2) is a heterodimeric enzyme present in bacteria (*1*), plants (*2*), and mammals (*3*). In mammals, it is located on the exterior surface of cells and is composed of a membrane-bound large subunit of 42 kDa, linked noncovalently to a small subunit of 20 kDa (*4*). In *Escherichia coli*, the large subunit is somewhat smaller (39 kDa) and the entire enzyme is present in the periplasmic space, currently constituting the only soluble form of the protein (*5*). GGT is responsible for the homeostasis of glutathione (GSH), its *in vivo* substrate, and plays an important role in cellular detoxification through the formation of mercapturic acids (3) and in conversion from leukotriene C_4 to D_4 (*6*). This enzyme is used as a hepatic marker for diagnosis of cirrhosis, although this has not been extensively exploited because of the presence of different isozymes in liver (*7*). GGT has also been shown to be involved in physiological disorders such as Parkinson's disease (*8*), apoptosis inhibition (*9*,*10*), diabetes, and cardiovascular diseases (*11*).

GGT catalyzes the cleavage of GSH (its *in vivo* acyl-donor substrate) between the γ-glutamyl and the cysteinylglycine moieties to form a covalent γ-glutamyl acyl-enzyme intermediate (Scheme 1) (*12*). In the subsequent hydrolysis reaction, a water molecule reacts with the intermediate to release glutamate. In the transpeptidation reaction, an amino acid or dipeptide can react with this intermediate as an acyl-acceptor substrate to form a di- or tripeptide product. The mechanisms of both reactions have been studied extensively by our group and others, especially for the enzyme purified from rat kidneys (*3*, *12*−*15*). The covalent nature of the acyl-enzyme intermediate has thus been demonstrated, and some amino acids were shown to be implicated in a general acid−base catalytic mechanism. For the *E. coli* GGT, purified in high yield from the periplasmic space, Thr391 was shown to be the active site nucleophile by inactivation of the enzyme with a mechanism-based inhibitor, followed by mass spectrometric characterization (*16*). This residue, located at the N-terminus of the small subunit, has also been shown to be involved in the autoactivation process of the enzyme (*17*). Recently, the X-ray structures of two bacterial forms of the enzyme have contributed greatly to our current understanding

† This work was carried out with the financial support of NSERC Discovery Grants to J.W.K. and P.T. R.C. and C.L. acknowledge NSERC and the Université de Montréal, respectively, for graduate bursaries. The authors acknowledge the Natural Sciences and Engineering Research Council of Canada (NSERC) and the Canadian Institutes of Health Research (CIHR) for financial support.

* Address correspondence to this author: Département de chimie, Université de Montréal, C.P. 6128, Succ. Centre-ville, Montréal (Québec), Canada H3C 3J7. Tel: (514) 343-6219. Fax: (514) 343-7586. E-mail: jw.keillor@umontreal.ca.

[1] Abbreviations: AMC, 7-amino-4-methylcoumarin; BMGY, buffered glycerol-complex medium; BMMY, buffered methanol-complex medium; GGT, γ-glutamyltranspeptidase; hGGT, human γ-glutamyltranspeptidase; GPNA, L-γ-glutamyl-*p*-nitroanilide; GSH, glutathione; His-tag, hexahistidine tag; YPD, yeast-peptone-dextrose culture media.

10.1021/bi700956c CCC: $37.00
Published on Web 10/09/2007

Scheme 1: Modified Ping-Pong Catalytic Cycle of GGT-Mediated Hydrolysis and Transpeptidation

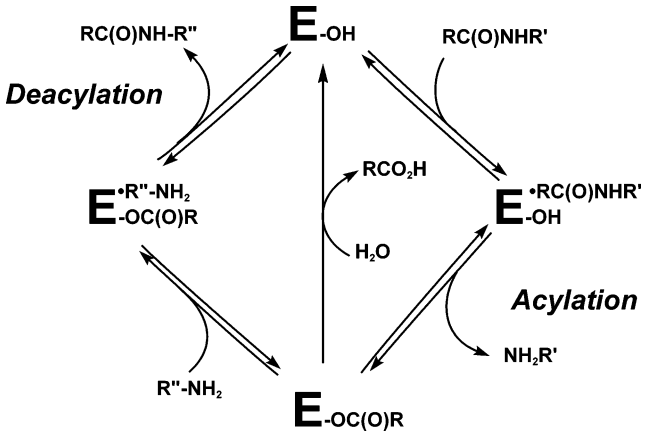

of GGT function. The structure of the acyl-enzyme intermediate of the *E. coli* enzyme confirmed the role of Thr391 and the location of the donor substrate binding site (*18*). Structural evidence has also been provided for the autocatalytic processing of the *E. coli* enzyme (*19*), and the recent structure of *Helicobacter pylori* GGT has shed still more light on this mechanism (*20, 21*). However, these bacterial GGTs have been shown to react poorly with amino acid acceptor substrates, underlining a fundamental difference compared to mammalian enzymes. This emphasizes the importance of further kinetic and structural studies with the mammalian enzymes, to determine the mechanisms and relative importance of the transpeptidation and hydrolysis reactions they catalyze (*1*, *20*).

In order to obtain critical structural and kinetic data, relatively large quantities of mammalian enzyme are required. Currently, the enzyme is isolated primarily from tissue (kidney, liver), typically involving the partial proteolytic digest of its anchor domain to release it from the membrane (*22*). A recombinant form of the rat enzyme has been expressed in *E. coli*, but only the relatively inactive precursor was obtained (*23*). The same enzyme expressed in *Saccharomyces cerevisiae* was capable of catalyzing transpeptidation, but it was produced in an impractically low yield (*24*). The human gene has been expressed with success in V79 and COS cells, but the manipulation of these cells is not straightforward, especially for potential site-directed mutagenesis experiments (*25, 26*). Highly active human GGT lacking the membrane anchor has been obtained following expression in *Sf21* cells and multistep purification. However, these cells grow slowly and are relatively tedious to manipulate (*27*). Therefore, we sought to develop a method for the facile expression and purification of human GGT.

In the present study, we present the cloning, expression, and purification of secreted human liver GGT by using *Pichia pastoris* as host system. Highly active purified human GGT was obtained in high yield by using a polyhistidine tag introduced at its C-terminus. The catalytic behavior of this new enzyme was characterized by UV−vis spectroscopy and mass spectrometry. The latter technique also allowed us to determine kinetic parameters for glutathione, the native but nonchromogenic substrate, for the first time. Incubation with an irreversible inhibitor, enzymatic digestion, and further structural analyses by mass spectrometry also allowed the first unambiguous identification of the active site nucleophile for the human enzyme, as well as characterization of N-linked glycans at several of the predicted sites. Finally, a homology model was generated to facilitate visualization of these structural and kinetic data.

MATERIALS AND METHODS

Chemicals. PCR solutions were purchased from New England Biolabs. Restriction enzymes and molecular markers for agarose gels were purchased from Fermentas. Primers for PCR amplifications were synthesized by AlphaDNA (Montreal, Canada). The plasmid pVL1392 containing the entire human liver GGT was obtained as a generous gift from Professor Taniguchi (Osaka University Medical School) (*27*). *Pichia pastoris* X-33 cells were kindly provided by Dr. Robert Lortie (IRC-CNRC, Montréal, Canada). All compounds necessary for the culture media LB, YPD, BMGY, and BMMY were purchased from BioShop (Montréal, Canada). Zeocin was obtained from Invitrogen. The salmon sperm DNA, casamino acids, protease inhibitors, GSH, γ-Glu-AMC, and buffers used in this study were purchased from Sigma-Aldrich. Ni-NTA resin was purchased from Qiagen. The Bradford concentrate solution and the solutions necessary for SDS−PAGE analysis were purchased from BioRad. The substrate L-γ-glutamyl-*p*-nitroanilide (GPNA) was synthesized according to the literature procedure (*13*). The irreversible inhibitor 2-amino-4-[mono(4-cyanophenyl)-phosphono]butanoic acid (Scheme 2) was kindly provided by Professor Hiratake (Kyoto University) (*28, 29*).

Cloning of hGGT. Amplification of the hGGT gene was performed by standard PCR procedures using the pVL1392 template encoding for the full sequence of the enzyme and Vent DNA Polymerase. The forward primer used was 5′-CACACAGAATTCTCAGCCTCCAAGGAACCT-3′ (with the *Eco*RI restriction site underlined), amplifying from residue 27 in the large subunit of hGGT (*30*), effectively truncating the membrane anchor sequence (*27*). The reverse primer used was 5′-CACACAGCGGCCGCGTAGCCG-GCAGGCTCCCC-3′ (with the *Not*I restriction site underlined). This amplified fragment was cloned into a pPICZαA plasmid (Invitrogen) by using the restriction sites inserted by the primers. The final plasmid was electrotransformed into *E. coli* XL-1 Blue cells, and the selection was controlled by using the antibiotic Zeocin in the media (25 μg/mL). The identity of the final plasmid, pPICZαA-hGGTΔ (Supporting Information, Figure S1), was verified by in-house sequencing (Département de biochimie, Université de Montréal).

Overexpression of Human GGT. The plasmid pPICZαA-hGGTΔ was transformed into *Pichia pastoris* X-33 cells by linearization of the DNA (~15 μg digested to completion by *Sac*I), precipitation by sodium acetate, and transformation by LiCl as described in manufacturer's protocols (Invitrogen). (Transformation into KM71H cells, that grow more slowly and can provide higher yields of recombinant protein, did not result in significant improvement in this case. Furthermore, the transformation of X-33 cells and plating at higher concentrations of Zeocin—to select for strains having incorporated more copies of the insertion plasmid—did not lead to substantial enhancement (*31*)). The genomic integration was verified according to standard protocols (Invitrogen) by isolation of genomic DNA from cultures of transformed X-33 and amplification of the hGGT gene with the primers

Scheme 2: Reaction of Hiratake's Phosphonate Inhibitor with Recombinant Human GGT

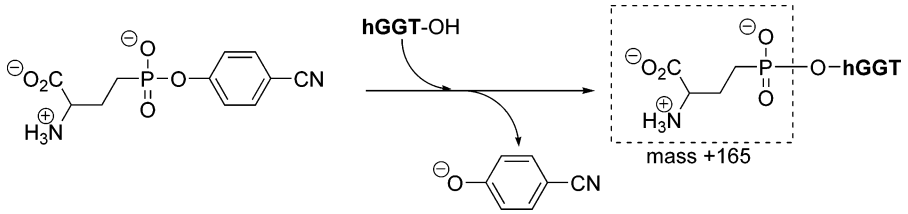

described above. The transformed strain (stable for months at −80 °C) was used to inoculate 10 mL of BMGY at 30 °C overnight. The culture was then centrifuged at 910*g* for 5 min at room temperature, and the pellet was resuspended in BMMY medium in order to give the desired final optical density (600 nm). Induction was carried out at 30 °C by addition of methanol every 24 h. These initial expression trials, based on the basic protocols in the manufacturer's manual, indicated that human GGT was indeed secreted into the supernatant, relative to the X-33 strain transformed with pPICZαA alone, as verified by the standard chromogenic activity assay using L-γ-glutamyl-*p*-nitroanilide and glycylglycine and by Bradford concentration assay (*22*). Subsequently, various aspects of the expression protocol were optimized:

The pH of the phosphate buffer present in BMGY and BMMY media was varied from 6.0 to 8.0. The use of media buffered at either pH 7.0 or pH 8.0 yielded hGGT having the highest specific activity, but some precipitation in the BMGY and BMMY media was observed at pH 8.0. Media buffered at pH 7.0 was therefore used for subsequent experiments.

Variation of the OD_{600} of the BMMY medium from 1.0 to 15.0 resulted in relatively little difference in the specific activity, but a small increase in the yield was observed after 90 h of induction, so an optical density of 15.0 prior to induction was retained for the final protocol. The addition of casamino acids from a 0.2 g/mL stock solution to give a final concentration of 1% in the BMMY medium was found to be the most important modification of the expression conditions. By adding 1% of casamino acids to the BMMY solution, even after only 20 h of induction, a significant increase in both the yield of hGGT and its specific activity was observed. The concentration of methanol used for induction was also varied. This aspect of the protocol is critical, since higher methanol concentration may result in more efficient expression, but can also be lethal for yeast. In our optimized protocol, culture to which 1% methanol was added every 24 h over 90 h provided the highest yield of GGT.

Purification of Human GGT. As described above, a volume of 10 mL of BMGY medium was inoculated with X-33 cells transformed with pPICZαA-hGGTΔ and was incubated with shaking (250 rpm) at 30 °C overnight. This culture was then used for the inoculation of 1 L of BMGY for 60 h. The cells were harvested and the cell pellet was resuspended in pH 7.0 BMMY medium containing 1% casamino acids to achieve a final OD_{600} of 15. The cells were then incubated with shaking (250 rpm) for 90 h at 30 °C with the addition of 1% methanol every 24 h. The culture was then centrifuged at 1500*g* for 20 min, and the pelleted cells were discarded. Concentration of 250 to 350 mL portions of the supernatant, containing the secreted, truncated human GGT, was necessary to allow efficient purification by Ni-NTA chromatography. Different techniques, including precipitation with ammonium sulfate or acetone, proved to be ineffective methods of concentration. Instead, ultrafiltration of 250 to 350 mL portions of the supernatant at 4 °C, using a stirring cell (Amicon) containing a membrane of 20−25 μm and a MWCO of 10 kDa, according to the manufacturer's procedures, proved to be successful. Buffer was exchanged through three successive washes with 100 mL portions of binding buffer (0.1 M potassium phosphate, pH 7.4), and the final resulting 35 mL portion of concentrate was then loaded onto Ni-NTA resin (Qiagen, 2 mL/L culture), washed with binding buffer (4 column volumes) and then with 5 and 10 mM imidazole (3 column volumes each), and finally eluted with buffer containing 250 mM imidazole (2 column volumes). Eluant fractions were desalted in 3 mL aliquots using 10-DG columns (BioRad) according to the manufacturer's instructions, eluting in 4 mL of 100 mM Tris-acetate buffer (pH 8.0). The protein was then concentrated at 4 °C to a final concentration of 1 mg/mL, using 10 kDa cutoff Amicon tubes (Millipore) and stored at −20 °C.

Determination of k_{cat} and K_M. Kinetic parameters for the substrate L-γ-glutamyl-*p*-nitroanilide (GPNA) were determined by varying its concentration between 0.1 and 3.5 mM in the presence of 20 mM of glycylglycine in the assay buffer (0.1 M Tris-HCl pH 8.0) at 37 °C. Around 8 mU of GGT were used in each kinetic run. The release of *p*-nitroaniline was followed at 410 nm. The initial rate−concentration data were analyzed by nonlinear least-squares regression according to the hyperbolic Michaelis−Menten equation. The apparent kinetic constants for the substrate glycylglycine were determined as above by varying its concentration between 0.5 and 20 mM in the presence of 1 mM of L-γ-glutamyl-*p*-nitroanilide at 37 °C. The V_{max} values were normalized for specific activity and transformed into k_{cat} values using a molecular weight of 61543 Da.

The apparent k_{cat} and K_M values for the transpeptidation substrates GSH and glycylglycine were determined by using 0.3−3.0 mM GSH in the presence of 1.0−30 mM glycylglycine in the same assay buffer, containing 22 μM of 7-(β-hydroxyethyl)theophylline as internal standard, at 37 °C with 40 mU of hGGT. For each GSH concentration, 250 μL aliquots were taken at time intervals ranging from 2 to 20 min, quenched with the addition of 75 μL of 40% TCA, and centrifuged at 10400*g* for 5 min to precipitate potential traces of protein. A series of seven γ-Glu-Gly-Gly standard solutions with concentrations ranging from 0.1 mM to 3 mM, spiked with the internal standard, were prepared as described above and used to generate a calibration curve from which reaction product concentrations were determined. Reaction samples as well as standard solutions were analyzed by LC−MS. Separations were performed on an 1100 LC system

coupled to an ESI-MSD-TOF mass spectrometer (Agilent Technologies). The chromatographic column was a Gemini, 3 μm, C_6-Phenyl, 4.6 × 50 mm from Phenomenex heated at 45 °C and operated at 0.4 mL/min. A linear gradient of 2−90% (0.1% formic acid in acetonitrile) was used over 6 min for a total run time of 11 min. The mass spectrometer was operated in positive electrospray mode. Mass spectra were acquired from *m*/*z* 100 to 1200 with an acquisition cycle of 0.89 s. Peak integration was performed using Analyst software (Agilent/MDS Sciex), and the analyte/internal standard area ratio was used for determination of reaction product concentration. Kinetic parameters were determined as described above.

The kinetic parameters for GSH hydrolysis were measured as described above, following the formation of Cys-Gly, using 2.2 μM internal standard in 50 mM ammonium bicarbonate (pH 8.0) buffer. GSH concentration was varied from 5 to 100 μM, and reaction aliquots were taken up to 60 min incubation at 37 °C.

Time-Dependent Inactivation Assay. The irreversible inhibition of recombinant hGGT was followed under pseudo-first-order conditions with a continuous activity assay. Reactions were initiated by addition of enzyme to solutions of 1.0−4.0 mM 2-amino-4-[mono(4-cyanophenyl)phosphono]butanoic acid and 8 μM γ-Glu-AMC in 100 mM Tris-HCl (pH 8.0) at 25 °C. Time-dependent loss of activity was followed by measuring the concentration of released fluorescent product AMC (λ^{exc} = 350 nm, λ^{em} = 440 nm) as a function of time over 30 min, corresponding to 3−5 half-lives. Pseudo-first-order rate constants were calculated from the corresponding curves according to the following monoexponential equation:

$$[P] = [P]_\infty(1 - e^{-(k_{obs}t)})$$

where [P] and $[P]_\infty$ are the concentrations of product formed at a given time, *t*, and at infinite time, respectively. The rate constants thus measured were normalized for the specific activity of GGT and plotted against inhibitor concentration, showing linear dependence with no sign of saturation, as observed previously by Hiratake (*28*). The second-order rate constant for inactivation was thus calculated from the equation

$$k_{obs} = k_{on}[I]/(1 + [S]/K_M)$$

deriving from the mechanistic scheme

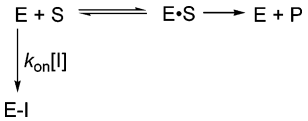

where [S] is the concentration of substrate γ-Glu-AMC (8 μM) and K_M is its Michaelis constant (12.6 μM (*28*)).

Identification of the Nucleophile of the Human GGT. Human GGT was incubated with 2 mM 2-amino-4-[mono-(4-cyanophenyl)phosphono]butanoic acid (Scheme 2) at 37 °C in the assay buffer for 20 min (Scheme 2). Protein samples were prepared at a concentration of 0.5 mg/mL in 50% acetonitrile, 1% formic acid. The mass of human GGT before and after reaction with the inhibitor was determined by LC−MS using an 1100 LC system coupled to a MSD-TOF mass spectrometer (Agilent Technologies). The chromatographic column was a Poroshell 300SB-C8, heated at 45 °C and operated at 0.2 mL/min. A linear gradient of 25−75% (0.1% formic acid in acetonitrile) over 10 min for a total run time of 15 min was used for elution. The mass spectrometer was operated in positive electrospray mode with a dual spray setup allowing for internal calibration and therefore offering very good mass accuracy. Mass spectra were acquired from *m*/*z* 110 to 2000 with an acquisition cycle of 0.89 s. Bioconfirm software (Agilent Technologies) was used to deconvolute the pattern of charge-state distributions of protein electrospray spectra.

To determine the residue labeled by the irreversible inhibitor, 50 μg of purified human GGT was incubated in 50 μL of 200 mM Tris-sulfate buffer pH 7.2 for 20 min in the absence and presence of 2 mM inhibitor and then digested in 4 M urea, 50 mM ammonium bicarbonate with Lys-C endopeptidase (Wako Chemicals, Richmond, VA) for 4 h at 37 °C. The digests were then diluted to 1 M urea with 50 mM ammonium bicarbonate prior to trypsin digestion (Promega trypsin, Fisher Scientific, Whitby, ON, Canada) overnight at 37 °C. All digests were analyzed by LC−MS−MS using a NanoAcquity system coupled to a Q-Tof Premier mass spectrometer (Waters Corporation). The chromatographic system comprised a Jupiter C_{18} 5 μm, 5 mm × 300 μm precolumn and a Jupiter C_{18} 3 μm, 10 cm × 150 μm analytical column (Phenomenex, Torrance, CA). The samples were initially transferred with an aqueous 0.1% formic acid solution to the precolumn with a flow rate of 4 μL/min for 5 min. Peptide elution was performed using a flow rate of 600 nL/min with a linear gradient of 10−60% (0.2% formic acid in acetonitrile) over 63 min. The mass spectrometer was operated in positive ion mode with a typical resolving power of at least 10,000 fwhm. The TOF analyzer of the mass spectrometer was externally calibrated with glufibrinopeptide B from *m*/*z* 50 to 1600. Mass spectra were acquired from *m*/*z* 400 to 1600 with an acquisition cycle of 2.3 s (1 s survey scan, 1 s MS−MS scan and 0.3 s interscan time). MS−MS spectra were collected using data-dependent acquisition for multiply charged ions exceeding 15 counts. A programmable collision energy ramp typically ranging from 30 to 80 eV (laboratory frame of reference) was used for precursor of different charge state to optimize fragment ion observation. Collision-induced dissociation was achieved using Ar as a collision gas.

Homology Model Generation. The homology model of human GGT was prepared using the PDB coordinates of the crystal structure of *E. coli* GGT (2DBU) as a template. The primary sequence of *E. coli* GGT was extracted from its crystal structure using the Homology module of InsightII (Accelrys, San Diego, CA) and aligned with the sequence of human GGT using either the Tcoffee server (*32*) or ClustalW (*33*), with default parameters. Five 3D models for human GGT were derived for each sequence alignment file using the crystal structure coordinates by Modeller 8v1 (*34*) with default parameters for generation of loop conformations. The quality of the proposed models was assessed using Whatcheck (*35*) and ProsaII (*36*). All ten models were then refined using a series of energy minimizations performed with the Discover module of InsightII. A tether restraint of 100 kcal/Å^2 was applied on all atoms, using 1000 steps of steepest descents minimization followed by a conjugate

gradients minimization until convergence of 0.001 kcal mol^{-1} $Å^{-1}$, with a distance-dependent dielectric constant of 4 to mimic the interior of proteins. The resulting structures were again analyzed using Molprobity, Whatcheck, and ProsaII, and one model was retained for refinement. It was then subjected to an unconstrained molecular dynamics simulation consisting of a 1 ps equilibration of the molecular system at 300 K, followed by simulated exploration of conformational space for 300 ps while maintaining the same temperature, using a nonbonding cutoff of 15 Å to speed the calculations.

RESULTS AND DISCUSSION

Purification of Recombinant Human GGT. The target hGGT was expressed, efficiently secreted, and subsequently purified according to the optimized protocols described above (see Materials and Methods). In this batch method, a quantity of 0.4 mg of enzyme having a specific activity of 237 U/mg was obtained, representing a yield of 86% for the one-step purification to apparent homogeneity by SDS−PAGE (Figure S2, Supporting Information). This is shown in Table S1 in Supporting Information, summarizing the purification protocol that provides an overall yield comparable to that reported for the enzyme expressed in *Sf21* insect cells, but with fewer manipulations (*27*). In the past, the purification of GGT has involved multiple size-exclusion, anion-exchange, or isoelectric-focusing chromatographic steps. Other protocols make use of antibodies raised against GGT or lectins that bind specifically to sugars present on the surface of the enzyme (*22*). However, to our knowledge, GGT has not previously been purified by immobilized metal ion affinity chromatography of active enzyme bearing a His-tag. While recombinant GGT bearing a His-tag has been expressed in the past, it was subsequently purified under denaturing conditions and used to raise antibodies (*37*). Thus, the current protocol permitting the expression of secreted, His-tagged, and active recombinant human GGT is clearly advantageous, and should allow facile subsequent mutagenesis studies.

Physical Characterization of Human GGT. In order to verify the integrity of human GGT, LC−MS experiments were performed. The large subunit eluted first, at 8.1 min (Figure 1a), and presented few different peaks at masses higher than the theoretical mass of the protein based on its amino acid sequence, 38489.8 Da. This heterogeneity was not unexpected as six Asn-glycosylation sites were predicted from its amino acid sequence. Moreover, three of these sites were confirmed as glycosylated by LC−MS−MS (see Figure 2). The main peaks observed in the mass spectrum of the large subunit are probably generated by the lack of one or more glycosylation moieties from heterogeneous glycosylation in *Pichia pastoris*. Importantly, the mass of these major peaks clearly indicates the absence of the N-terminal secretion factor, cleaved efficiently by the Kex2 protease, encoded by *Pichia pastoris* X-33 strain, at a recognition site present at the beginning of the large subunit of GGT (manufacturer's protocol).

The small subunit eluted at 8.6 min, and presented a major peak on its mass spectrum at 24918.6 Da (Figure 1c). This mass corresponds to the mass of 23052.8 Da predicted from its amino acid sequence, plus the difference due to glycosylation of Asn511 by $HexNAc_2$-Hex_9. Smaller peaks containing up to four additional hexose residues (different from each other by 162 Da) are also observed, due to heterogeneous glycosylation of Asn511 (see below).

The thermal denaturation of recombinant human GGT was also examined (see Supporting Information) and found to be identical to that of GGT purified previously from rat kidneys in our laboratory (*13*), showing the comparable stability of both enzymes.

Measurement of Kinetic Parameters. The apparent k_{cat} and K_M values of this new recombinant human GGT were obtained by using various concentrations of GPNA and glycylglycine as the donor and acceptor substrates, respectively. A K_M value of (614 ± 40) μM and a k_{cat} value of (76 ± 2) × 10^3 min^{-1} were obtained for the donor substrate in the presence of 20 mM GlyGly. As can be seen from Table 1, these values are comparable to those measured for the truncated human GGT (lacking a membrane anchor domain) purified from *Sf21* insect cells (2100 μM and 79 × 10^3 min^{-1}, respectively) (*27*) and for human GGT purified from human liver (K_M = 810 μM) (*38*) and kidney (k_{cat} = 69 × 10^3 min^{-1}) (*4*). Also obtained in this study were the K_M value of (6.3 ± 0.4) mM for glycylglycine and a k_{cat} of (60 ± 2) × 10^3 min^{-1} in the presence of 1 mM GPNA. These values also compare well with those reported previously in the literature of 3.4 mM and 42 × 10^3 min^{-1} for the hGGT expressed in insect cells (*27*) and a K_M value for glycylglycine of 12.4 mM with GGT isolated from human liver (*38*).

The similarity of the results obtained herein with those measured for the native enzyme isolated from tissue suggests that the presence of the C-terminal His-tag does not interfere with the activity of the enzyme. Thus, the recombinant human GGT secreted by yeast has physical and kinetic characteristics very similar to those published previously for recombinant GGT or GGT purified directly from tissue.

Kinetic constants were also measured for the natural substrate, GSH, using mass spectrometry. Since GSH does not contain a strong chromophore, other methods must be developed for detection of its reaction. These may include derivation methods (*39*), but mass spectrometry is also a powerful technique to apply to this problem. Recombinant hGGT was added to 30 mM GlyGly and varying concentrations of GSH and the reaction was quenched after various times up to 20 min. The concentration of product γ-Glu-Gly-Gly in each quenched aliquot was determined by LC−ESI-TOF (see Materials and Methods). In this way, an apparent K_M for GSH of (1.11 ± 0.29) mM and a k_{cat} of (13.4 ± 1.5) × 10^3 min^{-1} were obtained. It is interesting to note that this apparent k_{cat} value is ∼4-fold lower than that measured herein for GPNA transpeptidation (*vide supra*). This suggests that the activated substrate analogue GPNA reacts more quickly with GGT than its native substrate GSH, and is consistent with the acylation step being rate-limiting, as has been previously suggested (*13*). By way of further (although indirect) comparison, when the reaction of GSH and GlyGly with *rat* kidney GGT was studied by HPLC in our group, a K_M for GSH of 670 μM and a k_{cat} of 59.4 × 10^3 min^{-1} were obtained (*39*).

The concentration of acceptor substrate glycylglycine was also varied, as described in Materials and Methods. The variation of the concentrations of both GSH and glycylglycine provided initial rates that gave parallel lines on a double-reciprocal plot (see Figure S3 and Table S2 in Supporting

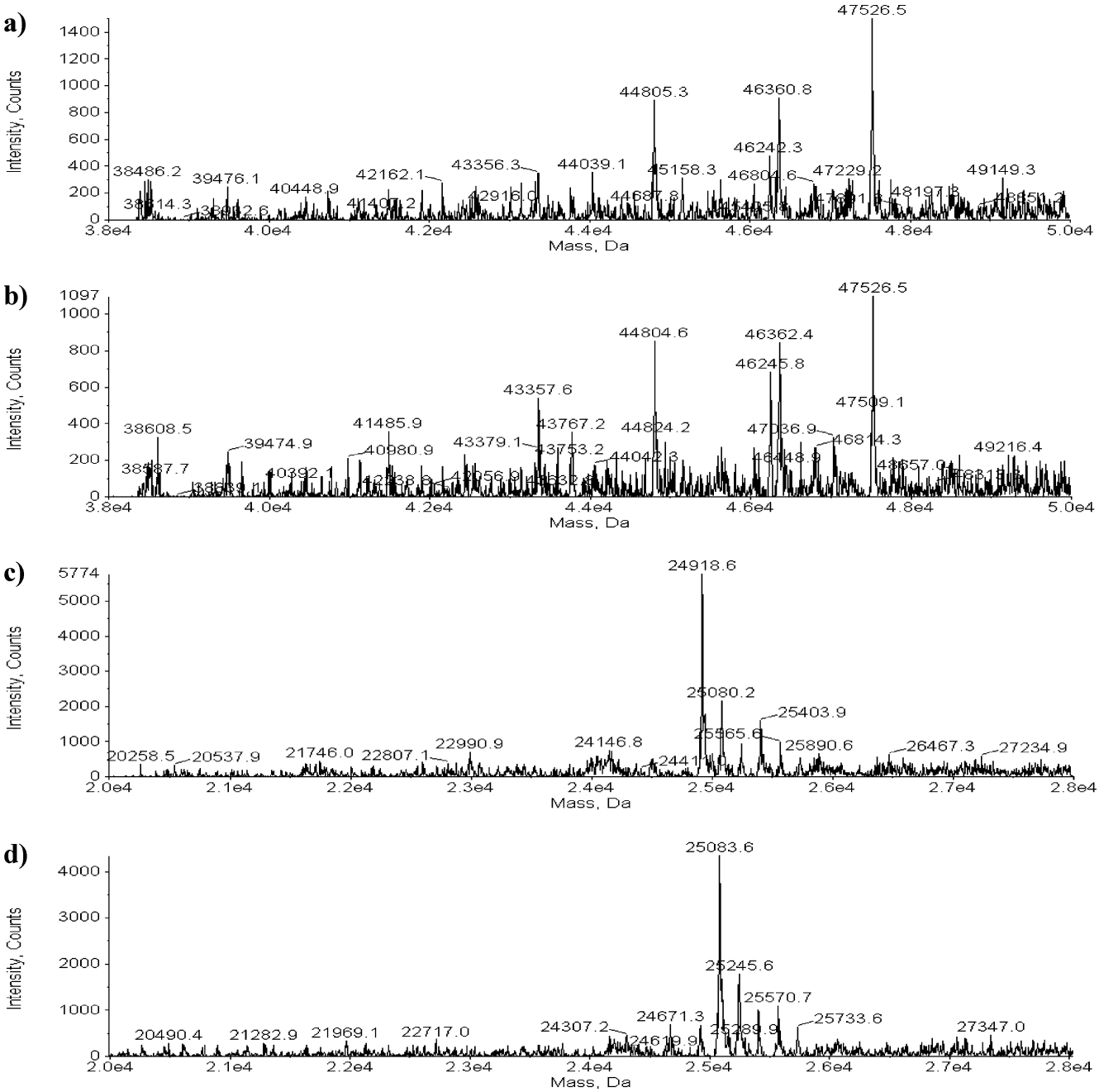

FIGURE 1: LC−MS analysis of hGGT large subunit (a) before and (b) after inactivation, and of hGGT small subunit (c) before and (d) after inactivation.

Information), consistent with the ping-pong mechanism shown in Scheme 1. When the concentration of donor substrate GSH was fixed at 3 mM (roughly 3-fold its apparent K_M value), an apparent K_M of (8.1 ± 0.8) mM was determined for glycylglycine. This value is similar to the apparent K_M value of (6.3 ± 0.4) mM measured at 1 mM GPNA (roughly 2-fold its apparent K_M value, *vide supra*). The comparison of these millimolar K_M values with the physiological concentrations of suitable amino acid or dipeptide acceptor substrates has elicited discussion regarding the physiological pertinence of the transpeptidation reaction (*40*, *41*). Furthermore, the low K_M values reported for either GSH or its S-conjugates for their *hydrolysis* are on the order of their physiological concentrations, suggesting that the primary role of GGT may be as a glutathione hydrolase (*40*, *41*). When the GGT-mediated hydrolysis of GSH was studied kinetically herein, the k_{cat} for GSH hydrolysis was found to be 53 ± 3 min^{-1} and the corresponding K_M value for GSH was determined to be 7.3 ± 1.9 μM (see Figure S4 in Supporting Information). This value is consistent with those measured previously for rat kidney GGT: measured at pH 8.0, it falls between the values of 5.7 μM, measured at pH 7.4 (*40*) and 8.8 μM (*40*) or 13.9 μM (*41*), measured at pH 8.5.

Identification of the Nucleophile of Human GGT. The expression protocol described above afforded easy access to quantities of enzyme required for stoichiometric labeling studies. Hiratake and co-workers have shown previously that phosphonate γ-glutamyl analogues can be used as mechanism-based irreversible inhibitors of GGT (*16*, *28*, *29*). When applied to the study of *E. coli* GGT, residue Thr391 at the N-terminus of the small subunit was identified as the catalytic

Truncated large subunit

```
 28  SASKEPDNHV YTRAAVAADA KQCSKIGRDA LRDGGSAVDA AIAALLCVGL   77
 78  MNAHSMGIGG GLFLTIYNST TRKAEVINAR EVAPRLAFAT MFNSSEQSQK  127
128  GGLSVAVPGE IRGYELAHQR HGRLPWARLF QPSIQLARQG FPVGKGLAAA  177
178  LENKRTVIEQ QPVLCEVFCR DRKVLREGER LTLPQLADTY ETLAIEGAQA  227
228  FYNGSLTAQI VKDIQAAGGI VTAEDLNNYR AELIEHPLNI SLGDAVLYMP  277
278  SAPLSGPVLA LILNILKGYN FSRESVESPE QKGLTYHRIV EAFRFAYAKR  327
328  TLLGDPKFVD VTEVVRNMTS EFFAAQLRAQ ISDDTTHPIS YYKPEFYTPD  377
378  DGG  380
```

Small subunit

```
381 *TAHLSVVAED GSAVSATSTI NLYFGSKVRS PVSGILFNNE MDDFSSPSIT  430
431  NEFGVPPSPA NFIQPGKQPL SSMCPTIMVG QDGQVRMVVG AAGGTQITTA  480
481  TALAIIYNLW FGYDVKRAVE EPRLHNQLLP NVTTVERNID QAVTAALETR  530
531  HHHTQIASTF IAVVQAIVRT AGGWAAASDS RKGGEPAGYA AASFLEQKLI  580
581  SEEDLNSAVD HHHHHH  596
```

FIGURE 2: Sequence of recombinant hGGT. Boxed residues are predicted N-X-S/T glycosylation sites; underlined residues are tryptic fragments identified by MS; bold residues are glycosylation sites observed by MS−MS (Asn120, Asn266, Asn344, and Asn511); the residue modified by the irreversible inhibitor (Thr381) is indicated with an asterisk.

Table 1: Comparison of Kinetic Constants Measured for Human GGT from Different Sources

	GPNA		GlyGly	
enzyme	k_{cat} (10^3 min^{-1})	K_M (μM)	k_{cat} (10^3 min^{-1})	K_M (mM)
expressed herein	76 ± 2[a]	614 ± 40[a]	60 ± 2[g]	6.3 ± 0.4[f]
expressed from *Sf21*[b]	79[c]	2100[c]	42[h]	3.4[h]
isolated from liver[d]	69[e]	810[f]	36[i]	12.4[j]

[a] Measured in the presence of 20 mM GlyGly. Relative errors derive from the nonlinear regression fitting to the Michaelis−Menten equation. [b] See ref 27. [c] Determined in the presence of 80 mM GlyGly. [d] See refs 4 and 38. [e] Calculated from the rate measured in the presence of 50 mM GlyGly and 2.5 mM GPNA (ref 4). [f] Determined at pH 7.6 in the presence of 50 mM GlyGly (ref 38). [g] Measured in the presence of 1 mM GPNA. Relative errors derive from the nonlinear regression fitting to the Michaelis−Menten equation. [h] Determined in the presence of 2 mM GPNA. [i] Calculated from the rate measured in the presence of 20 mM GlyGly and 1.0 mM GPNA, assuming a K_M value of 0.81 mM (ref 4). [j] Determined at pH 7.6 in the presence of 4 mM GPNA (ref 38).

nucleophile in the acyl-transfer reactions catalyzed by GGT and as a key residue for the autoactivation of the enzyme (*16*, *17*). As mentioned above, recent crystal structures of the *E. coli* and *H. pylori* enzymes confirm that this residue, conserved in every GGT known, is the catalytic nucleophile (*18*, *19*, *21*). However, no direct evidence has yet been provided for any eukaryotic enzyme.

The reaction of our recombinant human GGT with 2-amino-4-[mono(4-cyanophenyl)phosphono]butanoic acid (Scheme 2) was studied kinetically (see Supporting Information) according to the reaction conditions published originally by Hiratake (*28*). Our results confirm that human GGT is inhibited irreversibly by Hiratake's phosphonate and that this time-dependent inactivation is slowed in the presence of higher concentrations of donor substrate. Furthermore, the second-order rate constant for this inactivation was found to be 2.81 ± 0.14 M^{-1} s^{-1}, similar to Hiratake's value of 2.3 ± 0.1 M^{-1} s^{-1} measured for a commercial form of human GGT (*28*).

The incubation of recombinant hGGT with 2 mM 2-amino-4-[mono(4-cyanophenyl)phosphono]butanoic acid in pH 8.0 reaction buffer for 20 min thus led to its irreversible inhibition. Subsequent LC−MS analysis indicated that the major peaks of the large subunit remained unchanged (Figure 1b) while the mass pattern of the small subunit of inactivated GGT was shifted by +165 Da (Scheme 2, Figure 1d) relative to control enzyme. This corresponds to the addition of 1 equiv of the inhibitor phosphoryl group. After denaturation and digestion of similar samples of control and inactivated enzymes, the corresponding samples were analyzed by LC−MS−MS (see Materials and Methods), and the results obtained are shown in Figures 2 and 3. These experiments enabled protein sequence coverage of 53.7 and 73.6% of the small and large subunits, respectively (Figure 2). Notably, the N-terminal tryptic peptide of the inactivated small subunit was shifted by +165 Da, consistent with the covalent attachment of the inhibitor. Comparison of the MS−MS spectra of the N-terminal peptide from the inactivated (Figure 3a) and control (Figure 3b) GGT enabled the precise identification of the modification site. The cleavage of the labile inhibitor moiety was characterized by an abundant fragment ion at *m*/*z* 185, corresponding to the cleavage of the phosphoester bond, with concurrent transfer of the hydroxyl group and a proton from the adjoining Thr residue (Figure 3a). This loss of a water molecule from the Thr residue imparted a traceable −18 *m*/*z* shift on all N-terminal b-type fragment ions compared to the unmodified GGT (Figure 3b). These results unambiguously identified the N-terminus Thr381 residue as the binding site of the inhibitor and the active site nucleophile.

This unambiguous identification was possible due to the unique structure of Hiratake's phosphonate inhibitor that directs it to the active site nucleophile Thr381. By way of contrast, several irreversible inhibitors used in the past did not lead to identification of the active site nucleophile. For example, while L-diazoacetylserine (*42*), L-6-diazo-5-oxonorleucine (DON) (*42*, *43*), and acivicin (*43*−*46*) have been shown to label the small subunit of GGT, the autoprocessing of GGT was found to be unaffected by DON or acivicin (*43*). Furthermore, acivicin was shown to specifically label Thr-523 of the rat enzyme (*44*), Ser-405 of pig GGT (*45*), and the corresponding Ser-406 of human GGT (*43*). Mutagenesis studies also revealed that Ser-451 and Ser-452 are

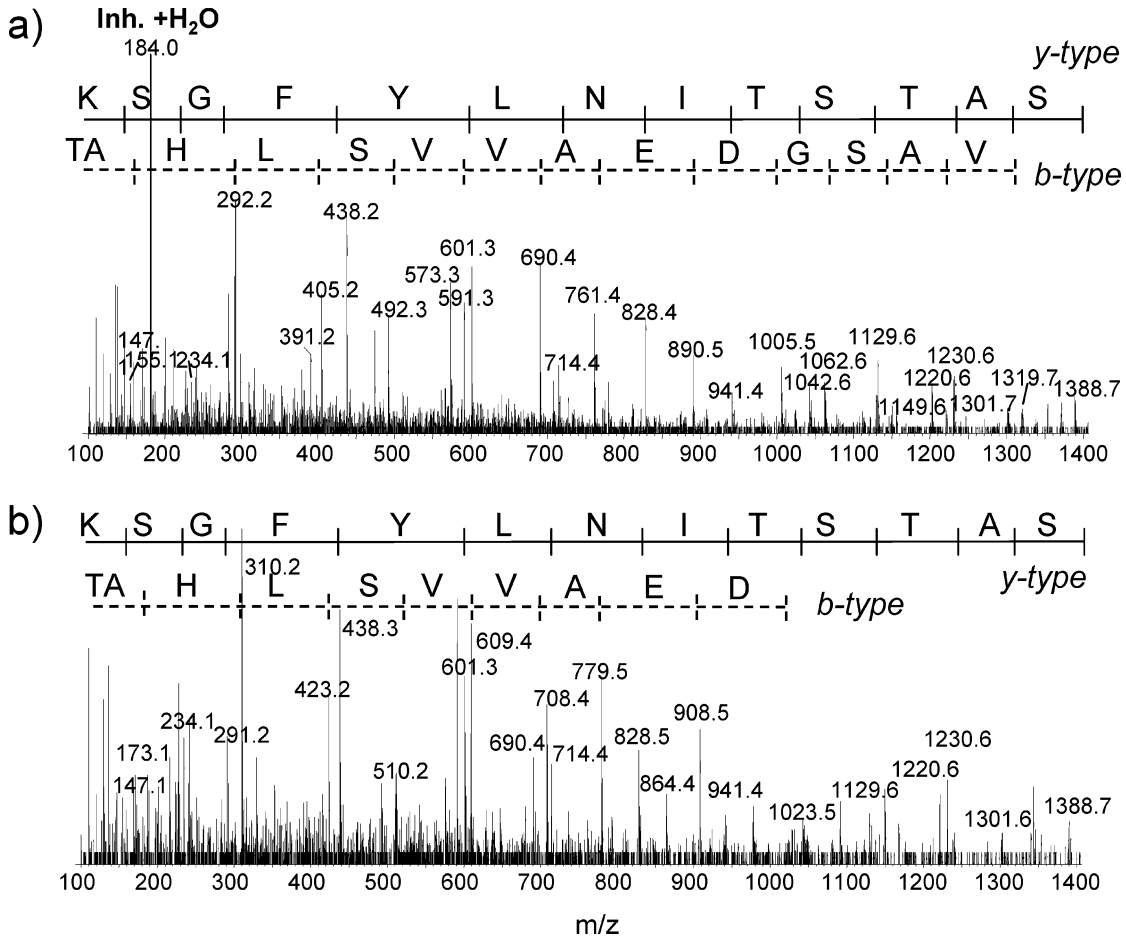

FIGURE 3: LC−MS−MS analyses of tryptic digests of hGGT. Tandem mass spectra of the N-terminal tryptic peptide 381−407 for the (a) inactivated and (b) control hGGT. Fragment ions corresponding to the cleavage of the amide bond with charge retention on the N- or C-terminal peptide segments are identified as b-type or y-type ions, respectively.

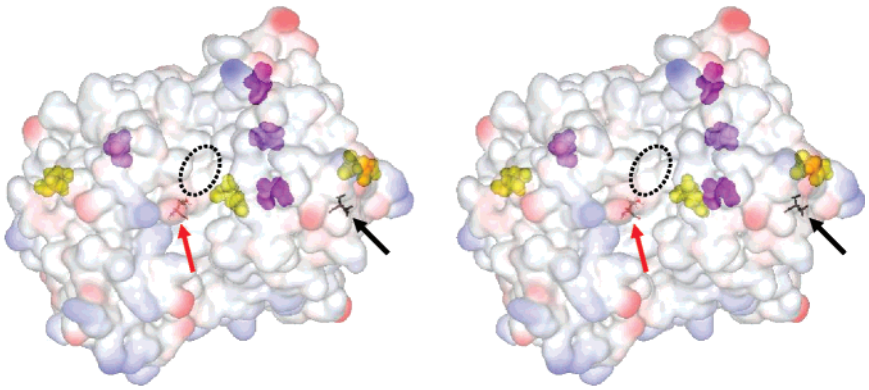

FIGURE 4: Relaxed-eyes stereoview of human GGT homology model. The active site nucleophile Thr381 is shown in stick form, indicated with a red arrow, with the γ-glutamyl binding site encircled in a dashed line. Shown in black stick form, indicated with a black arrow, is the N-terminal residue to which the membrane anchor domain would be attached in the full-length enzyme. N-linked glycosylation sites are identified in space fill form; those whose glycosylation sequences were determined herein are shown in purple while the others are shown in yellow.

required for reactivity of the human enzyme with acivicin. While the latter serine residues have been implicated in the binding of the carboxylate of the γ-glutamyl group of GSH (*18*), in our homology model, Ser-406 is located on the edge of active site, but some 14 Å distant from the active site nucleophile, while Thr-524 is on the same face of the enzyme, but 30 Å away. Moreover, subsequent mutation of both Ser-406 and the corresponding Thr-524 in the human enzyme yielded mutants that retained their activity (*43*). Taken together, it seems clear that acivicin is not bound in the γ-glutamyl pocket of GGT, at least in the same orientation as the donor substrate (*18*). In this context, Hiratake's phosphonate inhibitor distinguishes itself through its reaction with the active site nucleophile, presumably due to its careful design to closely resemble the γ-glutamyl donor substrate, if not the tetrahedral intermediate that it forms (*28*, *29*).

Human GGT Glycosylation. Further insight into the pattern of glycosylation of our recombinant hGGT was also gained by LC−MS−MS analysis. As mentioned above, Asn511 of

the small subunit of hGGT was found to be heterogeneously glycosylated with $GlcNAc_2$-Hex_9 up to $GlcNAc_2$-Hex_{13}. The extra 4 Hex residues are probably related to glucose units coming from immature glycoforms, suggesting incomplete glucosidase I/II activity in the *Pichia pastoris* expression system used.

The large subunit may contain up to 6 glycosylation sites, of which three were confirmed by LC−MS−MS analysis (see Figure 2). Sequential analysis showed that Asn120 bears a $GlcNAc_2$-Hex_9 motif, whereas Asn266 displays either $GlcNAc_2$-Hex_9 or $GlcNAc_2$-Hex_{10} and Asn344 is glycosylated with either $GlcNAc_2$-Hex_9 or $GlcNAc_2$-Hex_{11}. This heterogeneity (see also Figures 1a and 1b) may give rise to the different isoforms observed by SDS−PAGE for the large subunit (Figure S2) and is probably also due to immature glycoforms. The three sites whose glycosylation sequences are unassigned may have been missed because of their poor ionization efficiency or because of their *m*/*z* ions falling outside of the scanning range.

Homology Model. In the absence of a crystal structure for human GGT, a homology model was generated, using the recent *E. coli* structure (*18*) as a template (see Materials and Methods). While this model does not circumvent the need for a high-resolution structure of mammalian GGT, it does allow the visualization of the acylation and glycosylation sites identified herein (Figure 4). The identified active site nucleophile Thr381 is shown in stick form in Figure 4, adjacent to the previously identified γ-glutamyl binding site (*18*). The glycosylation sites identified and sequenced herein are shown in purple space-fill form, whereas those whose glycosylation sequences are unassigned are shown in yellow space-fill form. As is evident from Figure 4, all of the glycosylation sites shown through the semi-transparent surface are found in one hemisphere of the generally globular structure. This glycosylated half of the enzyme is opposite to the N-terminal membrane anchor (shown in black stick form) normally found in the full-length native protein. This is highly suggestive of the orientation of native GGT, sitting on the surface of a cell membrane, with its glycosyl groups extending into solution and its active site open to bind GSH.

SUMMARY

In summary, we have developed a protocol system for the expression and purification of highly active secreted human GGT by using *Pichia pastoris* as a host. This new expression system will allow the production of sufficient quantities of purified enzyme to permit further structural and kinetic study of the amino acid residues involved in transpeptidation and hydrolysis reactions catalyzed by the enzyme. In this work, the kinetic characterization of the recombinant enzyme with respect to its *in vivo* substrate, GSH, established the micromolar K_M value for the hydrolysis of GSH and the millimolar K_M value of glycylglycine as an acceptor substrate for transpeptidation *via* a ping-pong mechanism. Importantly, mass spectrometric analysis provided insight into the pattern of glycosylation of the small and large subunits and enabled, for the first time, the direct confirmation of Thr381, the N-terminal residue of the small subunit, as the catalytic nucleophile of human GGT. A homology model of human GGT was generated that allowed the visualization of the sites of acylation and glycosylation. The localization of glycosylation sites on the hemisphere of the enzyme containing the active site is suggestive of the orientation of the enzyme on the cell surface.

ACKNOWLEDGMENT

The authors thank Prof. N. Taniguchi (Osaka University Medical School) for the gift of plasmid pVL1392 harboring human fetal liver GGT, Prof. J. Hiratake (Kyoto University) for the phosphonate inhibitor, and Prof. Chartrand and Nicolas Paquin (Université de Montréal) for their invaluable technical assistance.

SUPPORTING INFORMATION AVAILABLE

Experimental details and graphical representation of kinetic data. This material is available free of charge via the Internet at http://pubs.acs.org.

REFERENCES

1. Suzuki, H., Kumagai, H., and Tochikura, T. (1986) gamma-Glutamyltranspeptidase from *Escherichia coli* K-12: purification and properties, *J. Bacteriol. 168*, 1325−1331.
2. Martin, M. N., and Slovin, J. P. (2000) Purified gamma-glutamyl transpeptidases from tomato exhibit high affinity for glutathione and glutathione S-conjugates, *Plant Physiol. 122*, 1417−1426.
3. Taniguchi, N., and Ikeda, Y. (1998) gamma-Glutamyl transpeptidase: catalytic mechanism and gene expression, *Adv. Enzymol. Relat. Areas Mol. Biol. 72*, 239−278.
4. Tate, S. S., and Ross, M. E. (1977) Human kidney gamma-glutamyl transpeptidase. Catalytic properties, subunit structure, and localization of the gamma-glutamyl binding site on the light subunit, *J. Biol. Chem. 252*, 6042−6045.
5. Suzuki, H., Kumagai, H., and Tochikura, T. (1986) gamma-Glutamyltranspeptidase from *Escherichia coli* K-12: formation and localization, *J. Bacteriol. 168*, 1332−1335.
6. Anderson, M. E., Allison, R. D., and Meister, A. (1982) Interconversion of leukotrienes catalyzed by purified gamma-glutamyl transpeptidase: concomitant formation of leukotriene D4 and gamma-glutamyl amino acids, *Proc. Natl. Acad. Sci. U.S.A. 79*, 1088−1091.
7. Nemesànszky, E., and Lott, J. A. (1985) gamma-Glutamyltransferase and its isoenzymes: progress and problems, *Clin. Chem. 31*, 797−803.
8. Sian, J., Dexter, D. T., Lees, A. J., Daniel, S., Jenner, P., and Marsden, C. D. (1994) Glutathione-related enzymes in brain in Parkinson's disease, *Ann. Neurol. 36*, 356−361.
9. Djavaheri-Mergny, M., Accaoui, M.-J., Rouillard, D., and Wietzerbin, J. (2002) Gamma-glutamyl transpeptidase activity mediates NF-kappaB activation through lipid peroxidation in human leukemia U937 cells, *Mol. Cell. Biochem. 232*, 103−111.
10. Del Bello, B., Paolicchi, A., Comporti, M., Pompella, A., and Maellaro, E. (1999) Hydrogen peroxide produced during gamma-glutamyl transpeptidase activity is involved in prevention of apoptosis and maintainance of proliferation in U937 cells, *FASEB J. 13*, 69−79.
11. Lee, D.-H., Jacobs, Jr. D. R., Jr., Gross, M., Kiefe, C. I., Roseman, J., Lewis, C. E., and Steffes, M. (2003) Gamma-glutamyltransferase is a predictor of incident diabetes and hypertension: the Coronary Artery Risk Development in Young Adults (CARDIA) Study, *Clin. Chem. 49*, 1358−1366.
12. Allison, R. D. (1985) gamma-Glutamyl transpeptidase: kinetics and mechanism, *Methods Enzymol. 113*, 419−437.
13. Ménard, A., Castonguay, R., Lherbet, C., Rivard, C., Roupioz, Y., and Keillor, J. W. (2001) Nonlinear free energy relationship in the general-acid-catalyzed acylation of rat kidney gamma-glutamyl transpeptidase by a series of gamma-glutamyl anilide substrate analogues, *Biochemistry 40*, 12678−12685.
14. Keillor, J. W., Ménard, A., Castonguay, R., Lherbet, C., and Rivard, C. (2004) Pre-Steady State Kinetic Studies of Rat Kidney γ-Glutamyl Transpeptidase Confirm its Ping-Pong Mechanism, *J. Phys. Org. Chem. 17*, 529−536.
15. Castonguay, R., Lherbet, C., and Keillor, J. W. (2003) Kinetic studies of rat kidney gamma-glutamyltranspeptidase deacylation

reveal a general base-catalyzed mechanism, *Biochemistry 42*, 11504−11513.
16. Inoue, M., Hiratake, J., Suzuki, H., Kumagai, H., and Sakata, K. (2000) Identification of catalytic nucleophile of *Escherichia coli* gamma-glutamyltranspeptidase by gamma-monofluorophosphono derivative of glutamic acid: N-terminal Thr-391 in small subunit is the nucleophile, *Biochemistry 39*, 7764−7771.
17. Suzuki, H., and Kumagai, H. (2002) Autocatalytic processing of gamma-glutamyltranspeptidase, *J. Biol. Chem. 277*, 43536−43543.
18. Okada, T., Suzuki, H., Wada, K., Kumagai, H., and Fukuyama, K. (2006) Crystal structures of gamma-glutamyltranspeptidase from *Escherichia coli*, a key enzyme in glutathione metabolism, and its reaction intermediate, *Proc. Natl. Acad. Sci. U.S.A. 103*, 6471−6476.
19. Okada, T., Suzuki, H., Wada, K., Kumagai, H., and Fukuyama, K. (2007) Crystal Structure of the γ-Glutamyltranspeptidase Precursor Protein from *Escherichia coli*, *J. Biol. Chem. 282*, 2433−2439.
20. Boanca, G., Sand, A., and Barycki, J. J. (2006) Uncoupling the enzymatic and autoprocessing activities of *Helicobacter pylori* gamma-glutamyltranspeptidase, *J. Biol. Chem. 281*, 19029−19037.
21. Boanca, G., Sand, A., Okada, T., Suzuki, H., Kumagai, H., Fukuyama, K., and Barycki, J. J. (2007) Autoprocessing of *Helicobacter pylori* gamma-glutamyltranspeptidase leads to the formation of a threonine-threonine catalytic dyad, *J. Biol. Chem. 282*, 534−541.
22. Meister, A., Tate, S. S., and Griffith, O. W. (1981) Gamma-glutamyl transpeptidase, *Methods Enzymol. 77*, 237−253.
23. Angele, C., Wellman, M., Thioudellet, C., Guellaen, G., and Siest, G. (1989) Expression of rat renal gamma-glutamyltransferase cDNA in *Escherichia coli*, *Biochem. Biophys. Res. Commun. 160*, 1040−1046.
24. Angele, C., Oster, T., Visvikis, A., Michels, J.-M., Wellman, M., and Siest, G. (1991) Different constructs for the expression of mammalian gamma-glutamyltransferase cDNAs in *Escherichia coli* and in *Saccharomyces cerevisiae*, *Clin. Chem. 375*, 662−666.
25. Thioudellet, C., Oster, T., Wellman, M., and Siest, G. (1994) Molecular and functional characterization of recombinant human gamma-glutamyltransferase. Coupling of its activity to glutathione levels in V79 cells, *Eur. J. Biochem. 222*, 1009−1016.
26. Ikeda, Y., Fujii, J., and Taniguchi, N. (1993) Significance of Arg-107 and Glu-108 in the catalytic mechanism of human gamma-glutamyl transpeptidase. Identification by site-directed mutagenesis, *J. Biol. Chem. 268*, 3980−3985.
27. Ikeda, Y., Fujii, J., Taniguchi, N., and Meister, A. (1995) Expression of an active glycosylated human gamma-glutamyl transpeptidase mutant that lacks a membrane anchor domain, *Proc. Natl. Acad. Sci. U.S.A. 92*, 126−130.
28. Han, L., Hiratake, J., Tachi, N., Suzuki, H., Kumagai, H., and Sakata, K. (2006) Gamma-(monophenyl)phosphono glutamate analogues as mechanism-based inhibitors of gamma-glutamyl transpeptidase, *Bioorg. Med. Chem. 14*, 6043−6054.
29. Han, L., Hiratake, J., Kamiyama, A., and Sakata, K. (2007) Design, Synthesis, and Evaluation of γ-Phosphono Diester Analogues of Glutamate as Highly Potent Inhibitors and Active Site Probes of γ-Glutamyl Transpeptidase, *Biochemistry 46*, 1432−1447.
30. Sakamuro, D., Yamazoe, M., Matsuda, Y., Kangawa, K., Taniguchi, N., Matsuo, H., Yoshikawa, H., and Ogasawara, N. (1988) The primary structure of human gamma-glutamyl transpeptidase, *Gene 73*, 1−9.
31. Clare, J. J., Romanos, M. A., Rayment, F. B., Rowedder, J. E., Smith, M. A., Payne, M. M., Sreekrishna, K., and Henwood, C. A. (1991) Production of mouse epidermal growth factor in yeast: high-level secretion using *Pichia pastoris* strains containing multiple gene copies, *Gene 105*, 205−212.
32. Notredame, C., Higgins, D. G., and Heringa, J. (2000) T-Coffee: A novel method for fast and accurate multiple sequence alignment, *J. Mol. Biol. 302*, 205−217.
33. Thompson, J. D., Higgins, D. G., and Gibson, T. J. (1994) CLUSTAL W: improving the sensitivity of progressive multiple sequence alignment through sequence weighting, position-specific gap penalties and weight matrix choice, *Nucleic Acids Res. 22*, 4673−4680.
34. Sali, A., and Blundell, T. L. (1993) Comparative Protein Modelling by Satisfaction of Spatial Restraints, *J. Mol. Biol. 234*, 779−815.
35. Hooft, R. W. W., Vriend, G., Sander, C., and Abola, E. E. (1996) Errors in Protein Structures, *Nature 381*, 272.
36. Sippl, M. J. (1993) Recognition of Errors in 3-Dimensional Structures of Proteins, *Proteins 17*, 355−362.
37. Chevalier, C., Thiberge, J.-M., Ferrero, R. L., and Labigne, A. (1999) Essential role of *Helicobacter pylori* gamma-glutamyltranspeptidase for the colonization of the gastric mucosa of mice, *Mol. Microbiol. 31*, 1359−1372.
38. Huseby, N. E. (1977) Purification and some properties of gamma-glutamyltransferase from human liver, *Biochim. Biophys. Acta 483*, 46−56.
39. Morin, M., Rivard, C., and Keillor, J. W. (2006) gamma-Glutamyl transpeptidase acylation with peptidic substrates: free energy relationships measured by an HPLC kinetic assay, *Org. Biomol. Chem. 4*, 3790−3801.
40. McIntyre, T. M., and Curthoys, N. P. (1979) Comparison of the Hydrolytic and Transfer Activities of Rat Renal γ-Glutamyltranspeptidase, *J. Biol. Chem. 254*, 6499−6504.
41. Elce, J. S., and Broxmeyer, B. (1975) γ-Glutamyltransferase of Rat Kidney, *Biochem. J. 153*, 223−232.
42. Tate, S. S., and Meister, A. (1977) Affinity Labeling of γ-Glutamyl Transpeptidase and Location of the γ-Glutamyl Binding Site on the Light Subunit, *Proc. Natl. Acad. Sci. U.S.A. 74*, 931−935.
43. Suzuki, H., and Kumagai, H. (2002) Autocatalytic Processing of γ-Glutamyltranspeptidase, *J. Biol. Chem. 277*, 43536−43543.
44. Stole, E., Seddon, A. P., Wellner, D., and Meister, A. (1990) Identification of a Highly Reactive Threonine Residue at the Active Site of γ-Glutamyl Transpeptidase, *Proc. Natl. Acad. Sci. U.S.A. 87*, 1706−1709.
45. Smith, T. K., Ikeda, Y., Fujii, J., Taniguchi, N., and Meister, A. Different Sites of Acivicin Binding and Inactivation of γ-Glutamyl Transpeptidases, (1995) *Proc. Natl. Acad. Sci. U.S.A.* 92, 2360−2364.
46. Ikeda, Y., Fujii, J., Anderson, M. E., Taniguchi, N., and Meister, A. (1995) Involvement of Ser-451 and Ser-452 in the Catalysis of Human γ-Glutamyl Transpeptidase, *J. Biol. Chem. 270*, 22223−22228.

BI700956C